IEICE Proceeding Series

Zero-lag and group synchronization in neural networks

Judith Lehnert, Thomas Dahms, Eckehard Schöll

Vol. 1 pp. 66-69
Publication Date: 2014/03/17
Online ISSN: 2188-5079

2012 International Symposium on Nonlinear Theory and its Applications
NOLTA2012, Palma, Majorca, Spain, October 22-26, 2012

Zero-lag and group synchronization in neural networks

Judith Lehnert, Thomas Dahms, and Eckehard Schöll

Institut für Theoretische Physik, Technische Universität Berlin, Hardenbergstraße 36, 10623 Berlin, Germany
Email: lehnert@itp.tu-berlin.de, dahms@itp.tu-berlin.de, schoell@physik.tu-berlin.de

Abstract—In the brain, synchronization is a prominent phenomenon associated with several cognitive capacities as well as pathological states like Parkinson's disease or epilepsy. We study the stability of synchronization in delay-coupled neural networks with a master stability approach. In the case of identical nodes and a single delay time, zero-lag synchronization is always, i.e., independently of the particular delay time and coupling strength, stable in excitatory networks. Inhibition can introduce a phase transition to desynchronization, e.g., in small-world or random networks. We then extend the master stability approach to more complex synchronization patterns where the nodes are synchronized in groups with phase lags between these groups. The local dynamics of each group can differ. For example, this approach allows us to use different neuronal models, e.g., for excitatory and inhibitory neurons. Furthermore, time delays and coupling strengths between the different clusters can be chosen nonuniformly allowing for complex dynamics, like bursting patterns, within the synchronization manifold even in the case of identical nodes. We discuss the stability of such patterns. In the case of identical nodes, delay times and coupling strengths, for appropriate topologies we obtain multistability between several cluster states.

1. Introduction

Synchronization in the brain can be related to cognitive capacities [1] as well as to pathological conditions, e.g., epilepsy [2]. Therefore, there has been tremendous interest in the study of synchronization in neural networks [3, 4, 5, 6]. The master stability approach has been applied to the study of synchronization patterns independently of a specific network topology [7, 8, 9]. The brain is organized in different brain areas leading to different delay times between neurons of distant areas and neurons within the same area. Furthermore, various types of neurons exist, corresponding to different local dynamics. Therefore we propose that the master stability function for zero-lag and group synchronization [9, 10, 11] will be especially useful for investigating complex neural synchronization phenomena.

The characterization of stability of isochronous synchronization has been widely studied, and the ground-breaking work by Pecora and Carroll [12] which allows for a separation of network topology and local dynamics of the nodes was recently also applied to networks with delays in the links [13, 14, 15, 16, 17]. Such delay times can greatly change the synchronization properties and appear in many natural coupled systems. In neuronal networks delays play a role due to finite distances between interacting neurons, but also due to processing lags in the neurons.

For group and cluster synchronization, attempts have been made to treat stability within a master stability approach. Sorrentino and Ott [10] considered two groups of nodes governed by different local dynamics. Dahms et al. [11] have shown how this can be generalized to a higher number of groups and introduced multiple coupling matrices to lift the restriction of multipartite topologies. This makes the theory accessible for a wide range of topologies.

We shortly review zero-lag synchronization in neural networks in Sec. 2. After introducing the notion of cluster and group dynamics in Sec. 3, we show how stability can be analyzed using the master stability function in Sec. 4. Finally, the effect of different topologies, coupling types, and delay times is shown for neuronal networks in Sec. 5.

2. Zero-lag synchronization

In Ref. [9], zero-lag synchronization was studied using the master stability approach in a network of identical nodes with a single delay time and coupling strength. It was shown that in excitatory networks, zero-lag synchronization is stable independently of the delay time, the overall coupling strength, the network size, and the particular topology. The term *excitatory networks* refers to networks where the coupling between each pair of nodes has a positive sign, and thus all entries of the coupling matrix are positive. Introducing long range inhibitory links, i.e., coupling with a negative sign, in rings with excitatory coupling, yields a sharp transition to desynchronization as the number of links exceeds a critical value. In comparison to these small-world-like networks, random networks of excitatory links are much less susceptible to desynchronization via inhibition.

3. Cluster and group dynamics

In a network consisting of N identical nodes, we refer to group synchronization as a state where groups of nodes exist that show isochronous synchronization internally, but synchronization between these group does not occur, or is of non-isochronous type, i.e., there may be a phase lag between groups [18, 19]. Cluster synchronization describes

the special case that all nodes in the network–and not only the nodes within one group–are identical.

Assume the number of groups to be M, where $k = 1, \ldots, M$ numbers the individual groups. The dynamical variables of the nodes in each group are then given by $\mathbf{x}_i^{(k)} \in \mathbb{R}^{d_k}$ with $i = 1, \ldots, N_k$, where N_k denotes the number of nodes in the k-th group. The dimension d_k of the $\mathbf{x}_i^{(k)}$ is given by the particular node model, e.g., the two-dimensional FitzHugh-Nagumo model [9].

In general the dimension d_k of the nodes $\mathbf{x}_i^{(k)}$ may be different for each group k. Consequently, also the local dynamics $\mathbf{F}^{(k)}(\mathbf{x}_i^{(k)})$ can be different for each group, but must be identical for all nodes $i = 1, \ldots, N_k$ in a given group k. For example, consider a network of neurons, where one group contains inhibitory neurons and another group contains excitatory ones. The local dynamics will be different for each group, and depending on the model used to describe both types of neurons also the dimension of the node dynamics may be different.

Let $\sigma_A^{(k)}$ be the coupling strength for the coupling from the $(k-1)$-th to the k-th group. In the same sense, let $\mathbf{A}^{(k)}$ be an $N_{k-1} \times N_k$ coupling matrix, such that its entries $\{A_{ij}^{(k)}\}$ represent the coupling of node j (which is in the $(k-1)$-th group) to node i (which is in the k-th group). By this construction we obtain a multipartite topology in which one cluster has incoming links from only one neighbor while having outgoing links to another one. In order to be able to deal with more complex topologies beyond multipartite structures like, for instance, lattices [20, 21] or hierarchical networks, we introduce a second set of coupling matrices. The $N_{n_k} \times N_k$ coupling matrix $\mathbf{B}^{(k)}$ describes the coupling from the n_k-th to the k-th group. That is, the k-th group now receives input from two groups, $k-1$ and n_k. The coupling strength associated with $\mathbf{B}^{(k)}$ is $\sigma_B^{(k)}$. Without loss of generality we assume the row sums of the coupling matrices $\mathbf{A}^{(k)}$ and $\mathbf{B}^{(k)}$ to be unity, which corresponds to the condition of unity or constant row sum needed in the special case of complete isochronous synchronization [12].

As coupling schemes $\mathbf{H}^{(k)}$ we introduce $d_{k-1} \times d_k$ matrices, given that d_{k-1} and d_k are the dimensions of $\mathbf{x}_i^{(k-1)}$ and $\mathbf{x}_i^{(k)}$, i.e., the dimensions of the local dynamics in the $(k-1)$-th and k-th group, respectively. Note that, as a generalization, nonlinear coupling functions $\mathbf{H}^{(k)} : \mathbb{R}^{d_{k-1}} \to \mathbb{R}^{d_k}$ may also be used instead of matrices [12, 10].

Finally, we allow the coupling delays $\tau_A^{(k)}$ and $\tau_B^{(k)}$ to be different. A schematic diagram of the variables and matrices is shown in Fig. 1(a) for two groups. Here, $\mathbf{A}^{(1)}$ and $\mathbf{A}^{(2)}$ denote the coupling between groups, depicted by dashed arrows, and $\mathbf{B}^{(1)}$ and $\mathbf{B}^{(2)}$ represent the coupling within the groups, depicted by solid arrows. Nodes of one group are depicted in the same gray scale (color).

The dynamics of any single node in the network can then be described by the differential equation

$$\dot{\mathbf{x}}_i^{(k)} = \mathbf{F}^{(k)}[\mathbf{x}_i^{(k)}(t)]$$

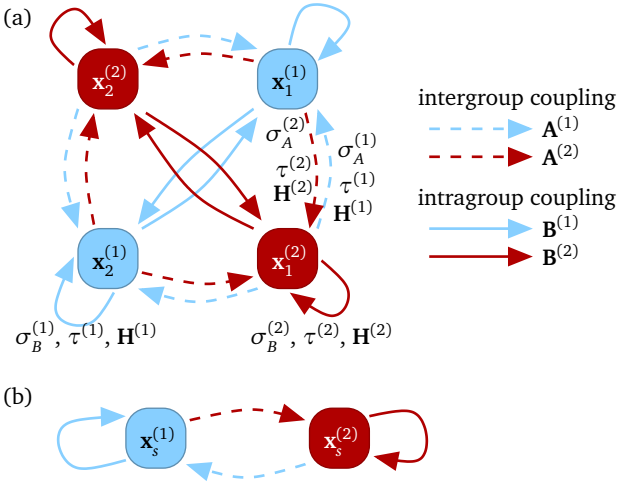

Figure 1: (Color online) (a) Schematic diagram of two groups visualizing parameters and dynamical variables as in Eq. (1). (b) The corresponding synchronization manifold according to Eq. (2).

$$+\sigma_A^{(k)} \sum_{j=1}^{N_{k-1}} A_{ij}^{(k)} \mathbf{H}^{(k)}[\mathbf{x}_j^{(k-1)}(t - \tau_A^{(k)}) - \mathbf{x}_i^{(k)}(t)]$$
$$+\sigma_B^{(k)} \sum_{j=1}^{N_{n_k}} B_{ij}^{(k)} \mathbf{H}^{(k)}[\mathbf{x}_j^{(n_k)}(t - \tau_B^{(k)}) - \mathbf{x}_i^{(k)}(t)], \quad (1)$$

for $i, j = 1, \ldots, N_k$, $k = 1, \ldots, M$, where we used a diffusive like coupling. The group synchronization manifold is then given by

$$\dot{\mathbf{x}}_s^{(k)} = \mathbf{F}^{(k)}[\mathbf{x}_s^{(k)}(t)] \quad +\sigma_A^{(k)} \mathbf{H}^{(k)}[\mathbf{x}_s^{(k-1)}(t - \tau_A^{(k)}) - \mathbf{x}_s^{(k)}(t)]$$
$$+\sigma_B^{(k)} \mathbf{H}^{(k)}[\mathbf{x}_s^{(n_k)}(t - \tau_B^{(k)}) - \mathbf{x}_s^{(k)}(t)], \quad (2)$$

which follows by inserting $\mathbf{x}_i^{(k)} = \mathbf{x}_j^{(k)} \equiv \mathbf{x}_s^{(k)}$ into Eq. (1) ($\forall i, j = 1, \ldots, N_k, \forall k = 1, \ldots, M$). For the example of two groups, Fig. 1(b) illustrates the synchronization manifold. Note that each group k may exhibit different synchronous dynamics. Even if the functions $\mathbf{F}^{(k)}$, the coupling matrices $\mathbf{H}^{(k)}$, and the delay times $\tau_A^{(k)}$ and $\tau_B^{(k)}$ are identical for each group, different initial conditions can lead to different dynamics. A generalization with more than two coupling terms is beyond the scope of this paper.

4. Stability of group synchronization

In order to investigate the stability of the synchronous state, we linearize Eq. (1) around the group synchronization manifold $\mathbf{x}_s^{(k)}$ ($k = 1, \ldots, M$):

$$\delta\dot{\mathbf{x}}_i^{(k)} = D\mathbf{F}^{(k)}(\mathbf{x}_s^{(k)})\delta\mathbf{x}_i^{(k)}$$
$$+\sigma_A^{(k)} \sum_{j=1}^{N_{k-1}} A_{ij}^{(k)} \mathbf{H}^{(k)}[\delta\mathbf{x}_j^{(k-1)}(t - \tau_A^{(k)}) - \delta\mathbf{x}_i^{(k)}(t)]$$

$$+\sigma_B^{(k)} \sum_{j=1}^{N_{n_k}} B_{ij}^{(k)} \mathbf{H}^{(k)}[\delta \mathbf{x}_j^{(n_k)}(t-\tau_B^{(k)}) - \delta \mathbf{x}_i^{(k)}(t)] \quad (3)$$

We can introduce block coupling matrices $\mathbf{Q}_A$ and $\mathbf{Q}_B$ including all inter-group coupling matrices. Let $\mathbf{Q}_A$ be the matrix containing the blocks $\mathbf{A}^{(kn)}$ at positions $(k, k-1)$, i.e.,

$$\mathbf{Q} = \begin{pmatrix} 0 & \cdots & \cdots & 0 & \mathbf{A}^{(1)} \\ \mathbf{A}^{(2)} & 0 & \cdots & \cdots & 0 \\ 0 & \mathbf{A}^{(3)} & 0 & \cdots & 0 \\ 0 & \ddots & \ddots & \ddots & 0 \\ 0 & \cdots & 0 & \mathbf{A}^{(M)} & 0 \end{pmatrix}, \quad (4)$$

and $\mathbf{Q}_B$ the matrix containing the blocks $\mathbf{B}^{(k)}$ at positions (k, n_k). If $\mathbf{Q}_A$ and $\mathbf{Q}_B$ commute, i.e., $[\mathbf{Q}_A, \mathbf{Q}_B] = 0$, it is possible to obtain a master stability equation

$$\begin{aligned} \delta\dot{\bar{\mathbf{x}}}^{(k)} &= \mathbf{D}\mathbf{F}^{(k)}(\mathbf{x}_s^{(k)})\delta\bar{\mathbf{x}}^{(k)}(t) \\ &+\sigma_A^{(k)}\gamma^{(1)}\mathbf{H}^{(k)}[\delta\bar{\mathbf{x}}^{(k-1)}(t-\tau_A^{(k)}) - \delta\bar{\mathbf{x}}^{(k)}(t)] \\ &+\sigma_B^{(k)}\gamma^{(2)}\mathbf{H}^{(k)}[\delta\bar{\mathbf{x}}^{(n_k)}(t-\tau_B^{(k)}) - \delta\bar{\mathbf{x}}^{(k)}(t)], \quad (5) \end{aligned}$$

for $k = 1, \ldots, M$, where $\gamma^{(1)}$ and $\gamma^{(2)}$ are chosen from the eigenvalue spectrum of the matrices matrices $\mathbf{Q}_A$ and $\mathbf{Q}_B$, respectively. These eigenvalues have to be evaluated in pairs corresponding to one eigenvector. Since $\mathbf{Q}_A$ and $\mathbf{Q}_B$ commute they always have a set of identical eigenvectors.

The largest Lyapunov exponent Λ calculated from Eq. (5) as a function of the complex parameters $\gamma^{(1)}$ and $\gamma^{(2)}$ is called the master stability function [12, 10, 11].

5. Group synchronization in neural networks

Here we apply our method to a neural network where the nodes are modeled as FitzHugh-Nagumo (FHN) systems. We consider a network of two groups coupled via two coupling matrices $\mathbf{Q}_A$ (intergroup coupling) and $\mathbf{Q}_B$ (intragroup coupling). The local dynamics of the i-th node in the k-th cluster is given as follows:

$$\mathbf{F}(\mathbf{x}_i^{(k)}) = \begin{pmatrix} \frac{1}{\epsilon}(u_i^{(k)} - \frac{1}{3}u_i^{(k)3} - v_i^{(k)}) \\ u_i^{(k)} + a \end{pmatrix} \quad (6)$$

with $\mathbf{x}_i^{(k)} = (u_i^{(k)}, v_i^{(k)})$ and $k = 1, 2$. Here u and v denote the activator and inhibitor variables, respectively. The parameter a determines the threshold of excitability. A single FHN oscillator is excitable for $a > 1$ and exhibits self-sustained periodic firing beyond the Hopf bifurcation at $a = 1$. We will focus on the excitable regime with $a = 1.3$. The timescale parameter ϵ is chosen as $\epsilon = 0.01$. We assume the coupling scheme $\mathbf{H}^{(1)} = \mathbf{H}^{(2)} \equiv \mathbf{H} = \begin{pmatrix} 1/\epsilon & 0 \\ 0 & 0 \end{pmatrix}$.

The dynamics within the synchronization manifold is equivalent to a system of two coupled nodes with self-feedback; cf. Fig. 1(b). In Ref. [22] it was shown that depending on the delay times, the coupling strength, and the strength of the self-feedback different dynamical scenarios, i.e., in-phase synchronization, anti-phase synchronization, or bursting can arise. Figure 2 shows the master stability function in panels (a)-(c) for in-phase synchronization, anti-phase synchronization and for synchronization in two bursting groups, respectively. The right hand panels of Fig. 2 depict the corresponding time series: In panel (d), (f), and (h) for the activator and in panel (e), (g), and (i) for the inhibitor for in-phase, anti-phase, and bursting dynamics, respectively. Because the different dynamical scenarios yield distinctively different stable regions, topologies might arise which show stable synchronization for one of the patterns but not for the others. However, for all scenarios the stable region contains the unity square, i.e., $(\gamma^{(1)}, \gamma^{(2)}) \in [-1, 1] \times [-1, 1]$. With Gershgorin's circle theorem [23] it can easily be shown that the eigenvalues of symmetrical matrices with positive entries and unity row sum are always contained in the interval $[-1, 1]$. Thus, if $\mathbf{Q}_A$ and $\mathbf{Q}_B$ have only positive entries, i.e., if the coupling is excitatory, synchronization is stable for the dynamics and parameters shown here. As a consequence, only the introduction of inhibitory links can lead to desynchronization as discussed in Sec. 2 above for the case of zero-lag synchronization. A detailed study of these phenomena for the eight-dimensional parameter space of $\sigma_A^{(k)}, \sigma_B^{(k)}, \tau_A^{(k)}, \tau_B^{(k)}$ $(k = 1, 2)$ is beyond the scope of this paper.

As an example of a network with inhibitory links which will exhibit stable synchronization in only one of the patterns discussed above, but not in the other ones, we choose

$$\mathbf{Q}_A = \begin{pmatrix} 0 & \mathbf{A} \\ \mathbf{A} & 0 \end{pmatrix}, \; \mathbf{Q}_B = \begin{pmatrix} \mathbf{B} & 0 \\ 0 & \mathbf{B} \end{pmatrix}, \quad (7)$$

where $\mathbf{A} = a_{ij}$ with $a_{ij} = 1 \; \forall i, j = 1, \ldots, N$ is an all-to-all coupling matrix with self-coupling. The choice of $\mathbf{Q}_B$ corresponds to $n_1 = 1$ and $n_2 = 2$; cf. Sec. 3. $\mathbf{B}$ is an undirected random matrix with both excitatory (positive entries) and inhibitory links (negative entries). The matrix $\mathbf{B}$ describes a network with a fixed node degree with 12 excitatory and 9 inhibitory links for each node. The number of nodes is chosen as $N = 100$. The black dots in Fig. 2 denote the corresponding eigenvalue pairs. In panels (a) and (b) some eigenvalues are located outside the stable region, while in panel (c) they are all inside, which means that the zero-lag and anti-phase synchronized solutions will be unstable in such a network, while synchronization in the bursting state will be stable.

6. Conclusion

Based on a master stability approach, we have studied patterns of cluster and group synchronization in delay-coupled networks and determined their stability. Using multiple commuting coupling matrices, we have generalized the stability analysis beyond multipartite topologies, for instance towards lattices or hierarchical network structures. As a concrete example we have focused on a neu-

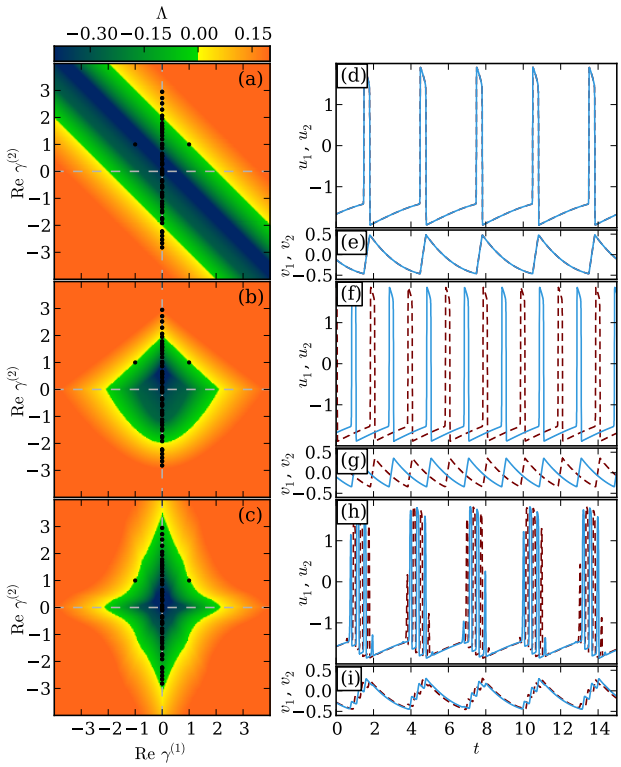

Figure 2: (Color online) (a)-(c): Master stability function for networks of FitzHugh-Nagumo oscillators governed by Eq. (6). The black dots denote the location of the eigenvalue pairs for the example topology (7). (d)-(i): Time series of the dynamics in the first (dark dashed red) and second (light solid blue) group. Parameters: (a),(d),(e): in-phase synchronization ($\tau_B^{(k)} = 3$), (b),(f),(g): anti-phase synchronization ($\tau_B^{(k)} = 2$), (c),(h),(i): synchronized bursting ($\tau_B^{(k)} = 3.2$). Other Parameters: $\sigma_A^{(k)} = \sigma_B^{(k)} = 0.5, \tau_A^{(k)} = 3, \epsilon = 0.01, a = 1.3$ (groups $k = 1, 2$).

ral networks and the interplay of different delay times and topology, which is a step towards understanding complex patterns of synchronization in real-world networks.

Acknowledgments

This work was supported by DFG in the framework of SFB 910.

References

[1] W. Singer, Neuron **24**, 49 (1999).

[2] P. J. Uhlhaas and W. Singer, Neuron **52**, 155 (2006).

[3] S. Coombes and C. Laing, Phil. Trans. R. Soc. A **367**, 1117 (2009).

[4] W. Lu and T. Chen, IEEE Trans. Circuits Syst. I **51**, 2491 (2004).

[5] M. Timme, T. Geisel, and F. Wolf, Chaos **16**, 015108 (2006).

[6] P. Uhlhaas, G. Pipa, B. Lima, L. Melloni, S. Neuenschwander, D. Nikolic, and W. Singer, Front. Integr. Neurosci. **3**, 17 (2009).

[7] M. Dhamala, V. K. Jirsa, and M. Ding, Phys. Rev. Lett. **92**, 074104 (2004).

[8] V. K. Jirsa, Cogn. Neurodyn. **2**, 29 (2008).

[9] J. Lehnert, T. Dahms, P. Hövel, and E. Schöll, Europhys. Lett. **96**, 60013 (2011).

[10] F. Sorrentino and E. Ott, Phys. Rev. E **76**, 056114 (2007).

[11] T. Dahms, J. Lehnert, and E. Schöll, Phys. Rev. E (2012), in print (arXiv:1203.4916).

[12] L. M. Pecora and T. L. Carroll, Phys. Rev. Lett. **80**, 2109 (1998).

[13] W. Kinzel, A. Englert, G. Reents, M. Zigzag, and I. Kanter, Phys. Rev. E **79**, 056207 (2009).

[14] A. Englert, W. Kinzel, Y. Aviad, M. Butkovski, I. Reidler, M. Zigzag, I. Kanter, and M. Rosenbluh, Phys. Rev. Lett. **104**, 114102 (2010).

[15] V. Flunkert, S. Yanchuk, T. Dahms, and E. Schöll, Phys. Rev. Lett. **105**, 254101 (2010).

[16] S. Heiligenthal, T. Dahms, S. Yanchuk, T. Jüngling, V. Flunkert, I. Kanter, E. Schöll, and W. Kinzel, Phys. Rev. Lett. **107**, 234102 (2011).

[17] V. Flunkert and E. Schöll, New. J. Phys. **14**, 033039 (2012).

[18] C. U. Choe, T. Dahms, P. Hövel, and E. Schöll, Phys. Rev. E **81**, 025205(R) (2010).

[19] A. A. Selivanov, J. Lehnert, T. Dahms, P. Hövel, A. L. Fradkov, and E. Schöll, Phys. Rev. E **85**, 016201 (2012).

[20] J. Kestler, W. Kinzel, and I. Kanter, Phys. Rev. E **76**, 035202 (2007).

[21] J. Kestler, E. Kopelowitz, I. Kanter, and W. Kinzel, Phys. Rev. E **77**, 046209 (2008).

[22] E. Schöll, G. Hiller, P. Hövel, and M. A. Dahlem, Phil. Trans. R. Soc. A **367**, 1079 (2009).

[23] M. G. Earl and S. H. Strogatz, Phys. Rev. E **67**, 036204 (2003).